

SHORT PAPER

Inferring sleep stage from local field potentials recorded in the subthalamic nucleus of Parkinson's patients

Elijah Christensen^{1,2}  | Aviva Abosch³ | John A. Thompson^{3*}  |
Joel Zylberberg^{1,4*} 

¹Department of Physiology and Biophysics, University of Colorado School of Medicine, Aurora, Colorado

²Medical Scientist Training Program, University of Colorado School of Medicine, Aurora, Colorado

³Department of Neurosurgery, University of Colorado School of Medicine, Aurora, Colorado

⁴Computational Biosciences Program, University of Colorado School of Medicine, Aurora, Colorado

Correspondence

Elijah Christensen, Department of Physiology and Biophysics, University of Colorado School of Medicine, Aurora, CO.
Email: elijah.christensen@ucdenver.edu

Funding Information

This research was supported by funds from the Boettcher Foundation Webb-Waring Biomedical Research Awards program (JAT), Sloan Research Fellowship (JZ), CIFAR Azrieli Global Scholar Award (JZ), Google Faculty Research Award (JZ), and investigator-initiated funding for prior data collection used in this study (AA).

Abstract

Parkinson's disease (PD) is highly comorbid with sleep dysfunction. In contrast to motor symptoms, few therapeutic interventions exist to address sleep symptoms in PD. Subthalamic nucleus (STN) deep brain stimulation (DBS) treats advanced PD motor symptoms and may improve sleep architecture. As a proof of concept toward demonstrating that STN-DBS could be used to identify sleep stages commensurate with clinician-scored polysomnography (PSG), we developed a novel artificial neural network (ANN) that could trigger targeted stimulation in response to inferred sleep state from STN local field potentials (LFPs) recorded from implanted DBS electrodes. STN LFP recordings were collected from nine PD patients via a percutaneous cable attached to the DBS lead, during a full night's sleep (6–8 hr) with concurrent polysomnography (PSG). We trained a feedforward neural network to prospectively identify sleep stage with PSG-level accuracy from 30-s epochs of LFP recordings. Our model's sleep-stage predictions match clinician-identified sleep stage with a mean accuracy of 91% on held-out epochs. Furthermore, leave-one-group-out analysis also demonstrates 91% mean classification accuracy for novel subjects. These results, which classify sleep stage across a typical heterogeneous sample of PD patients, may indicate spectral biomarkers for automatically scoring sleep stage in PD patients with implanted DBS devices. Further development of this model may also focus on adapting stimulation during specific sleep stages to treat targeted sleep deficits.

KEYWORDS

artificial neural network, deep brain stimulation, Parkinson's disease, sleep dysfunction, subthalamic nucleus

1 | INTRODUCTION

Sleep is crucial to the regulation of physiological and cognitive functions in humans, and when disordered greatly diminishes quality of life (Giuditta et al., 1995; Pace-Schott & Hobson, 2002) and adversely affects nervous system repair (Brager et al., 2016; Lucke-Wold et al., 2015). Parkinson's disease (PD) is a neurodegenerative

disorder that exhibits a high degree of comorbidity with a wide range of sleep disorders (De Cock, Vidailhet, & Arnulf, 2008; Tekriwal et al., 2017). The diagnosis and treatment of PD primarily focus on the overt motor symptoms (Postuma et al., 2015). However, there is increasing interest in understanding the impact of non-motor symptoms, such as sleep dysfunction, on overall disease burden (Chaudhuri, Healy, & Schapira, 2006), and in identifying treatments for these symptoms. With the onset of motor fluctuations or breakthrough tremor despite optimal medical management, subthalamic

*Co-senior authors who made equal contributions to this work.

nucleus (STN) deep brain stimulation (DBS) surgery has become the reference standard for treating the motor symptoms of advanced PD (Bronstein et al., 2011; Hamani, Saint-Cyr, Fraser, Kaplitt, & Lozano, 2004). Interestingly, several studies have found that STN-DBS can improve sleep in PD (Arnulf et al., 2000; De Cock et al., 2011; Iranzo, Valldeoriola, Santamaría, Tolosa, & Rumià, 2002). In our previous work, using local field potentials (LFPs) recorded from DBS electrodes implanted in STN for the treatment of PD, we identified unique spectral patterns within STN oscillatory activity that correlated with distinct sleep cycles, a finding that might offer insight into sleep dysregulation (Thompson et al., 2018). One extension of this work was to determine whether LFP information recorded from the STN could be used in real time to objectively identify sleep cycles for targeted therapy using DBS. In other words, the sleep benefit derived from STN stimulation could potentially be optimized using an adaptive stimulation algorithm that is aimed at specific sleep stages. In this study, we demonstrate the use of a feedforward artificial neural network that predicts sleep stage from LFP recordings, within the STN, with high precision.

2 | MATERIALS AND METHODS

2.1 | Patient demographics

This study was approved by the Institutional Review Board of the University of Minnesota, where the surgical and recording procedures were performed. All consenting study subjects ($n = 9$) carried a diagnosis of idiopathic PD (Figure 1a). Subjects were unilaterally implanted in the STN with a quadripolar DBS electrode (model

#3389; Medtronic Inc., Fridley, MN), per routine surgical protocol (Abosch et al., 2012). Experimental details for the recording setup have been previously published (Thompson et al., 2018). Basic characterization of these data was previously reported in Thompson et al. (2018).

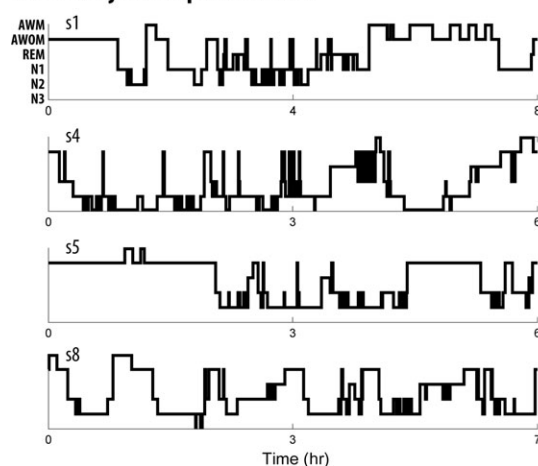
2.2 | Signal processing of local field potentials

Signal processing of the raw STN LFP signals was previously described in Thompson et al. (2018). Briefly, after preprocessing, the four LFP channels (0, 1, 2 and 3; one recording from each of the four electrical contacts of the implant) were converted into three bipolar derivations (LFP01, LFP12 and LFP23) by sequentially referencing them. Power spectral density (PSD) was estimated using a fast Fourier transform from a 2-s-long sliding window (Hamming) with 1-s overlap. The final time-evolving spectra had 15 s time and 0.5 Hz frequency resolution. For each subject, LFP data selected for further analysis were based on the location of the DBS electrode contact within the STN and this was verified by the following: (a) intraoperative microelectrode recordings that identified cells with firing characteristics consistent with STN neurons; (b) anti-Parkinsonian benefit and side-effects of macrostimulation; (c) preoperative stereotactic T1- and T2-weighted images merged to a postoperative MRI demonstrating the position of the DBS electrode within the borders of STN; (d) the use of Framelink (Medtronic Corp.) software to analyse DBS position on the postoperative MRI; and (e) evaluation of the efficacy of post-programming stimulation for contralateral motor symptoms for each subject (Ince et al., 2010). Selection of which contact(s) to use for study recordings was based on the STN contact

(a) PD subject demographics ($n = 9$)

	Age (y)	PD Dur. (y)	% Improv.	30 second sleep epochs (#)					
				Total	Awake	REM	N1	N2	N3
mean	60.11	10.67	61.89	837.11	377.89	62.29	134.78	186.00	88.40
median	61.00	9.50	61.00	791.00	282.00	73.00	106.00	221.00	10.00
std	9.56	4.63	11.40	165.67	246.58	45.61	94.79	122.20	112.90
min	39	6	47	676	97	11	33	3	4
max	70	19	79	1149	850	133	284	322	239
range	31	13	32	473	753	122	251	319	235

(b) PD subject sleep architecture



(c) Spectral power by sleep stage

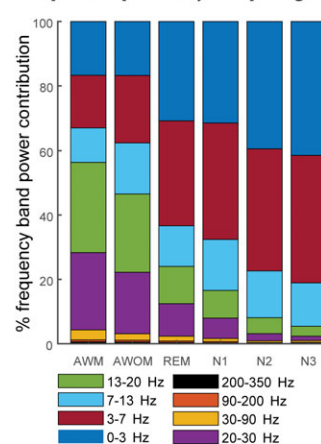


FIGURE 1 (a) Demographic data and sleep stage characteristics for Parkinson's disease (PD) subjects participating in this study ($n = 9$). Percent improvement in PD reflects the change in the Unified Parkinson's Disease Rating Scale (UPDRS) motor scale before and after DBS surgery. (b) Hypnograms from four representative subjects in this study, indicative of common sleep architecture deficits reported for individuals with PD. (c) Distribution of frequency band power contribution to sleep stage for all subjects. AWM, awake with movement; AWOM, awake without movement; REM, rapid eye movement

(s) associated with peak beta-spectrum activity as this feature correlates with the optimal programming contact(s) for the treatment of contralateral motor symptoms (Ince et al., 2010). These criteria were used to ensure that the selected contact was most reliably in the same relative anatomical location across patients to permit generalizability of the model.

2.3 | Video-PSG scoring

The polysomnographic electrode montage used was the following: F3–C3, P3–O1, F4–C4 and P4–O2, EOG1–A2, EOG2–A1, and chin EMG (Iber, Ancoli-Israel, Chesson, & Quan, 2007). Sleep stages were determined by analysis of 30-s epochs of the PSG, by a sleep neurologist, with each epoch classified as Awake or as belonging to one of the following sleep stages: rapid eye movement (REM), or the non-REM (NREM) stages of N1, N2 or N3.

2.4 | Model description

We trained a feedforward artificial neural network (ANN) with a single hidden layer (Figure 2b) to prospectively identify whether a given 30-s epoch of STN-LFP recording took place during one of three possible states: REM, NREM or Awake. Inputs to the model were eight separate frequency band power bins, averaged over 30 s: delta (0–3 Hz), theta (3–7 Hz), alpha (7–13 Hz), low beta (13–20 Hz), high beta (20–30 Hz), and low gamma (30–90 Hz), high gamma (90–200) and high frequency oscillations (200–350). Each frequency range input feature was normalized independently by subtracting the mean and scaling by the variance of feature. The ANN output is a probability that the measured epoch occurs during one of the three possible states. Optimal ANN architecture was chosen based on the hyperparameter optimization detailed below. The ANN model utilizes a single hidden layer to encode the normalized spectral power bands

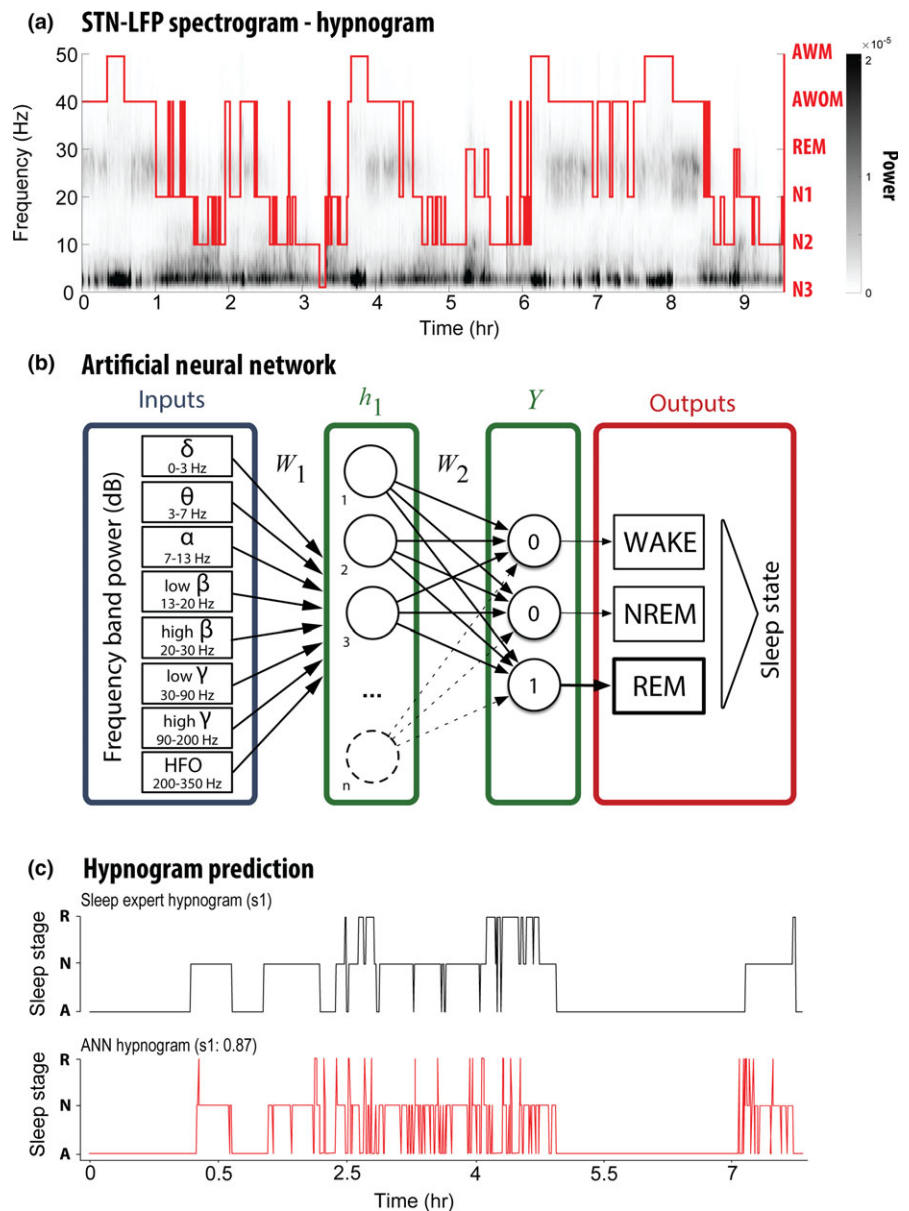


FIGURE 2 (a) Representative spectrogram of a local field potential (LFP) recording acquired over the course of one full night's sleep from a deep brain stimulation (DBS) electrode implanted into the subthalamic nucleus (STN). A PSG-informed hypnogram assessed by a sleep expert is aligned with the LFP recordings (red line; AWM, awake with movement; AWOM, awake without movement; REM, rapid eye movement; N1–3, non-rapid eye movement stages 1–3). (b) Schematic representation of the feedforward classifier used to predict sleep stage from 30-s labelled LFP epochs. The model is composed of an input layer (LFP frequency power bands), a hidden layer and an output layer (predicted sleep stage). (c) Comparison of hypnogram assessed by a sleep expert (top; black) and ANN-predicted hypnogram (bottom; red) from patient 1 with mean classification accuracy of 87%

within 32 features by calculating weighted sums of the input frequency power and scaling them by a non-linear function. Weighted linear combinations of these 32 features are then used by the network to compute sleep state probabilities with application of a soft-max non-linearity.

2.5 | Hyperparameter optimization

The architecture of the ANN model we describe was determined by evaluating classification accuracy across the spectrum of network hyperparameters. We combinatorically varied the non-linearity of each unit (Sigmoid, ReLu and Tanh), the number of units in the

hidden layer(s) (16, 32 or 64) and the number of hidden layers (1 or 2). Randomly initialized models in replicates of five were each trained and tested on a random 80:20 partition of all data. In general, we observed that more complex models with a larger number of total units and multilayer networks produced minor increases in classification accuracy, but these performance variations were not statistically significant. We opted to use 32 units in a single hidden layer with the biology-inspired rectified linear units (ReLU; (Hahnloser, Sarpeshkar, Mahowald, Douglas, & Seung, 2000)) as the non-linearity. We chose this configuration because it achieved classification accuracy on a par with the best-performing model with 10-fold fewer parameters to minimize overfitting training data.

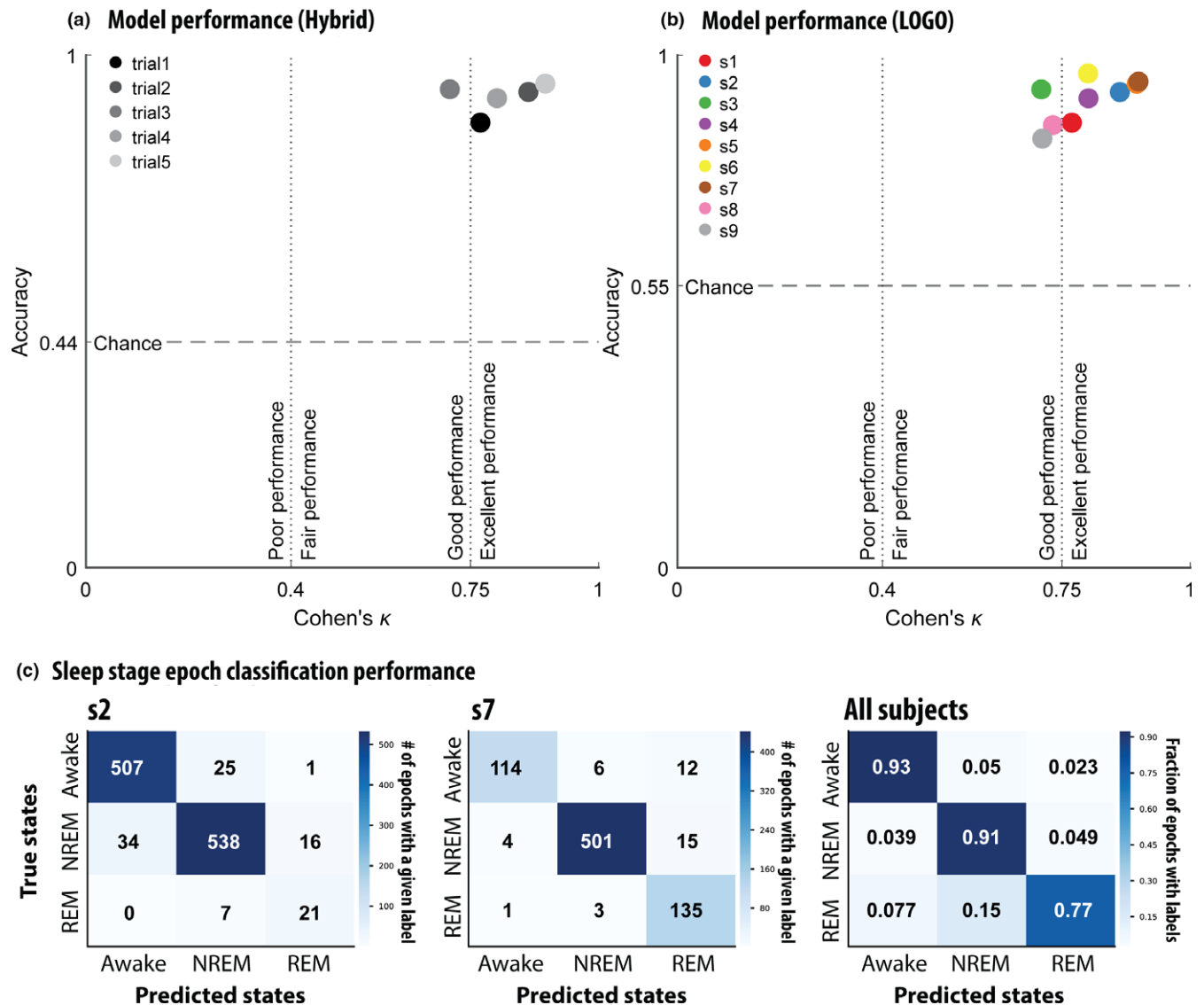


FIGURE 3 (a) In the “hybrid” strategy a random 80% of each patient's local field potential (LFP) recordings were pooled to train the model. Model accuracy and Cohen's κ were evaluated on the withheld 20% from each patient. This analysis was replicated in four other random 80:20 splits to control sampling bias. Cohen's κ magnitude guidelines derived from Fleiss & Cohen (1973). (b) A leave-one-group-out (LOGO) cross-validation strategy was used to test generalizability to unseen patients. Each data point represents a model trained with a specific patient excluded from its training data. Model accuracy and Cohen's κ were evaluated on data from the kept-out patient. (c) Confusion matrices of representative models trained using the LOGO cross-validation strategy. The first two confusion matrices represent individual subjects and the final confusion matrix depicts the fraction of epochs with specific class labels for all subjects. REM, rapid eye movement; NREM, non-rapid eye movement

3 | RESULTS

3.1 | Model performance and validation

We evaluated the ANN model's sleep stage classification performance and its ability to generalize new predictions under two conditions. Performance was evaluated using accuracy ($A_{\text{observed}} = \frac{\text{Correct}}{\text{Correct} + \text{Incorrect}}$) and Cohen's κ ($\kappa = \frac{A_{\text{observed}} - A_{\text{chance}}}{1 - A_{\text{chance}}}$). Chance accuracy (A_{chance}) was calculated as originally described (Cohen, 1960).

First, we tested the model's ability to predict sleep stages on novel examples from patients included in the training set. We pooled 80% of each patient's 30-s STN-LFP recording epochs across all nine patients to train the model. The remaining 20% of the withheld epochs were used to evaluate the model's performance on novel examples from familiar patients. The train-test fractions (80:20) were sampled randomly for each patient and performance was averaged in replicates of five to prevent sampling bias. The model was able to correctly predict sleep stage from STN-LFP epochs with a mean accuracy of 91% (Figure 3a).

Training a model from scratch for each new patient is often intractable. Therefore, the model's ability to perform well on never-seen subjects demonstrates its sensitivity to the salient spectral features of sleep across individual variations. To test this level of generalization, the model was trained on all epochs from eight of the nine patients. Subsequently, model performance was evaluated on all epochs from the kept-out patient. Thus, nine different models were trained, each with a specific patient withheld from its training data. As above, model performance was quantified using accuracy and Cohen's κ (Figure 3b). Across all models, mean classification accuracy of 91% was observed. Finally, because the number of epochs of each observed sleep state varies between patients in the dataset, we produced confusion matrices for the test patient of each model and show representative examples from patients with significantly imbalanced sampling as well as a summary matrix averaged across all models (Figure 3c). This demonstrates that the model's error rate varies as a function of sleep-stage representation, with less frequent stages showing a higher error rate (see Table 1).

4 | DISCUSSION

In this report, we demonstrate the novel use of an optimized ANN to predict sleep stage from 30-s epochs of LFP recorded from the STN of PD subjects. Based on results from hyperparameter optimization, we used a network architecture of a single hidden layer containing 32 artificial neurons with ReLU non-linearities (Figure 2b). We evaluated the model's ability to generalize to new patients by using a LOGO (leave-one-group-out) strategy for cross-validation and attained mean classification accuracy of 91% averaged across all patients.

The ability of this ANN model to accurately predict sleep stages based on STN-LFP data recorded from novel PD patients is a critical

TABLE 1 Summary for all subjects of the epoch representation and model accuracy for each of the following sleep stages: Awake, rapid eye movement (REM) and an aggregate of the non-rapid eye movement (NREM) substages (N1, N2 and N3)

Subject ID	Awake		NREM		REM	
	% of epochs	% correct	% of epochs	% correct	% of epochs	% correct
1	50	91	42	90	9	47
2	46	94	51	94	2	55
3	88	98	11	69	1	0
4	16	82	73	95	11	84
5	53	99	43	96	3	39
6	88	96	12	100	0	NA
7	17	96	66	98	18	83
8	27	94	61	85	12	83
9	40	96	60	100	0	NA

Percent correct values were derived from the leave-one-group-out analysis.

NA, not available.

improvement over our previously published effort to generate a predictive model. In our prior work, we used a support vector machine (SVM) model that performed well when tested on novel epochs derived from the familiar patient used to train the model but failed to generalize to novel subjects (Thompson et al., 2018). For simplification of model development, the different NREM stages (i.e. NREM 1–3) were aggregated into a single class. However, future development will focus on classification of the non-REM substages, as they represent distinct states and underlie unique sleep processes. Our current study is the first to use direct intracranial recordings from human basal ganglia to classify and match unseen PSG-labelled electrophysiological signals. Although the overall accuracy of the model for all sleep stages combined was well above chance (91%), performance on REM sleep stages was lower than the average performance (77%). Decreased performance for REM could be a result of the lower representation across subjects (see Table 1), or it may reflect the challenge in identifying the REM state from PSG in this patient population.

This model can be implemented in forthcoming improved DBS neurostimulators to detect sleep stage solely from features of STN-recorded LFP, enabling the implementation of closed-loop stimulation strategies for treating sleep dysregulation in PD patients. This would serve a crucial unmet need in this patient population (Chaudhuri et al., 2006), as there are currently no effective treatments with a low side-effect burden (Arnulf et al., 2000). Although DBS is an established therapy for the treatment of motor symptoms of Parkinson's disease, the effect of DBS on the sleep disturbances of Parkinson's disease has not yet been fully characterized, and the mechanism(s) underlying the improvements reported in sleep quality, efficiency and duration remains to be elucidated (Sharma, Sengupta, Chitnis, & Amara, 2018).

Our model's ability to correctly predict sleep stage in novel subjects may imply the existence of a universal LFP spectrum sleep

signature within STN. In our investigations to date, this STN localized spectral signature appears conserved across patient demographics, robust to variances in implantation location, and detectable from the aggregate activity of several thousands of neurons. In future work, we intend to characterize this spectral signature space using generative ANN models of LFP oscillations recorded from within the STN. This effort will extend our understanding of the relationship between sleep dynamics and oscillating field potentials in the basal ganglia.

ACKNOWLEDGEMENTS

We thank the subjects who participated in this study.

AUTHOR CONTRIBUTIONS

EC, JZ, JAT and AA were responsible for conception and design of the study. AA acquired the data. EC and JZ conceived the model and developed the code for its application. EC, JZ and JAT analyzed and interpreted the data. EC and JAT drafted the manuscript. EC, AA, JZ and JAT critically revised the manuscript.

ORCID

Elijah Christensen  <https://orcid.org/0000-0003-2166-1169>

John A. Thompson  <https://orcid.org/0000-0003-2991-5194>

Joel Zylberberg  <https://orcid.org/0000-0002-8208-5698>

REFERENCES

- Abosch, A., Lanctin, D., Onaran, I., Eberly, L., Spaniol, M., & Ince, N. F. (2012). Long-term recordings of local field potentials from implanted deep brain stimulation electrodes. *Neurosurgery*, *71*, 804–814. <https://doi.org/10.1227/neu.0b013e3182676b91>
- Arnulf, I., Bejjani, B. P., Garma, L., Bonnet, A. M., Houeto, J. L., Damier, P., ... Agid, Y. (2000). Improvement of sleep architecture in PD with subthalamic nucleus stimulation. *Neurology*, *55*, 1732–1734. <https://doi.org/10.1212/wnl.55.11.1732>
- Brager, A. J., Yang, T., Ehlen, J. C., Simon, R. P., Meller, R., & Paul, K. N. (2016). Sleep is critical for remote preconditioning-induced neuroprotection. *Sleep*, *39*, 2033–2040. <https://doi.org/10.5665/sleep.6238>
- Bronstein, J. M., Tagliati, M., Alterman, R. L., Lozano, A. M., Volkman, J., Stefani, A., ... Pahwa, R. (2011). Deep brain stimulation for Parkinson disease. *Archives of neurology*, *68*, 165–165.
- Chaudhuri, K. R., Healy, D. G., & Schapira, A. H. (2006). National Institute for clinical excellence non-motor symptoms of Parkinson's disease: Diagnosis and management. *The Lancet. Neurology*, *5*, 235–245.
- Cohen, J. (1960). A coefficient of agreement for nominal scales. *Educational and psychological measurement*, *20*, 37–46. <https://doi.org/10.1177/001316446002000104>
- De Cock, V. C., Debs, R., Oudiette, D., Leu, S., Radji, F., Tiberge, M., ... Dauvilliers, Y. (2011). The improvement of movement and speech during rapid eye movement sleep behaviour disorder in multiple system atrophy. *Brain*, *134*, 856–862. <https://doi.org/10.1093/brain/awq379>
- De Cock, V. C., Vidailhet, M., & Arnulf, I. (2008). Sleep disturbances in patients with parkinsonism. *Nature clinical practice. Neurology*, *4*, 254–266. <https://doi.org/10.1038/ncpneuro0775>
- Fleiss, J. L., & Cohen, J. (1973). The equivalence of weighted kappa and the intraclass correlation coefficient as measures of reliability. *Educational and psychological measurement*, *33*, 613–619. <https://doi.org/10.1177/001316447303300309>
- Giuditta, A., Ambrosini, M. V., Montagnese, P., Mandile, P., Cotugno, M., Zucconi, G. G., & Vescia, S. (1995). The sequential hypothesis of the function of sleep. *Behavioural brain research*, *69*, 157–166. [https://doi.org/10.1016/0166-4328\(95\)00012-i](https://doi.org/10.1016/0166-4328(95)00012-i)
- Hahnloser, R. H. R., Sarpeshkar, R., Mahowald, M. A., Douglas, R. J., & Seung, H. S. (2000). Erratum: Digital selection and analogue amplification coexist in a cortex-inspired silicon circuit. *Nature*, *405*, 947–951. <https://doi.org/10.1038/35016072>
- Hamani, C., Saint-Cyr, J. A., Fraser, J., Kaplitt, M., & Lozano, A. M. (2004). The subthalamic nucleus in the context of movement disorders. *Brain*, *127*, 4–20. <https://doi.org/10.1093/brain/awh029>
- Iber, C., Ancoli-Israel, S., Chesson, A., & Quan, S. (2007). *The AASM manual for the scoring of sleep and associates events: Rules, terminology and technical specifications*. Westchester, IL: American Academy of Sleep Medicine.
- Ince, N. F., Gupte, A., Wichmann, T., Ashe, J., Henry, T., Bebler, M., ... Abosch, A. (2010). Selection of optimal programming contacts based on local field potential recordings from subthalamic nucleus in patients with Parkinson's disease. *Neurosurgery*, *67*, 390–397. <https://doi.org/10.1227/01.neu.0000372091.64824.63>
- Iranzo, A., Valdeoriola, F., Santamaría, J., Tolosa, E., & Rumià, J. (2002). Sleep symptoms and polysomnographic architecture in advanced Parkinson's disease after chronic bilateral subthalamic stimulation. *Journal of Neurology, Neurosurgery and Psychiatry*, *72*, 661–664. <https://doi.org/10.1136/jnnp.72.5.661>
- Lucke-Wold, B. P., Smith, K. E., Nguyen, L., Turner, R. C., Logsdon, A. F., Jackson, G. J., ... Miller, D. B. (2015). Sleep disruption and the sequelae associated with traumatic brain injury. *Neuroscience & Biobehavioral Reviews*, *55*, 68. <https://doi.org/10.1016/j.neubiorev.2015.04.010>
- Pace-Schott, E. F., & Hobson, J. A. (2002). The neurobiology of sleep: Genetics, cellular physiology and subcortical networks. *Nature Reviews Neuroscience*, *3*, 591–605. <https://doi.org/10.1038/nrn895>
- Postuma, R. B., Berg, D., Stern, M., Poewe, W., Olanow, C. W., Oertel, W., ... Deuschl, G. (2015). MDS clinical diagnostic criteria for Parkinson's disease. *Movement disorders: Official journal of the Movement Disorder Society*, *30*, 1591–1601. <https://doi.org/10.1002/mds.26424>
- Sharma, V. D., Sengupta, S., Chitnis, S., & Amara, A. W. (2018). Deep brain stimulation and sleep-wake disturbances in Parkinson disease: A review. *Frontiers in neurology*, *9*, 697. <https://doi.org/10.3389/fneur.2018.00697>
- Tekriwal, A., Kern, D. S., Tsai, J., Ince, N. F., Wu, J., Thompson, J. A., & Abosch, A. (2017). REM sleep behaviour disorder: Prodromal and mechanistic insights for Parkinson's disease. *Journal of Neurology, Neurosurgery and Psychiatry*, *88*, 445–451. <https://doi.org/10.1136/jnnp-2016-314471>
- Thompson, J. A., Tekriwal, A., Felsen, G., Ozturk, M., Telkes, I., Wu, J., ... Abosch, A. (2018). Sleep patterns in Parkinson's disease: Direct recordings from the subthalamic nucleus. *Journal of Neurology, Neurosurgery and Psychiatry*, *89*, 95–104. <https://doi.org/10.1136/jnnp-2017-316115>

How to cite this article: Christensen E, Abosch A, Thompson JA, Zylberberg J. Inferring sleep stage from local field potentials recorded in the subthalamic nucleus of Parkinson's patients. *J Sleep Res*. 2018;e12806. <https://doi.org/10.1111/jsr.12806>